Contribution of the Active Site Histidine Residues of Ribonuclease A to Nucleic Acid Binding†

Chiwook Park,‡ L. Wayne Schultz,‡,§ and Ronald T. Raines*,‡,||

Department of Biochemistry and Department of Chemistry, University of Wisconsin−Madison, Madison, Wisconsin 53706

Received January 3, 2001

ABSTRACT: His12 and His119 are critical for catalysis of RNA cleavage by ribonuclease A (RNase A). Substitution of either residue with an alanine decreases the value of k_{cat}/K_M by more than 10^4-fold. His12 and His119 are proximal to the scissile phosphoryl group of an RNA substrate in enzyme−substrate complexes. Here, the role of these active site histidines in RNA binding was investigated by monitoring the effect of mutagenesis and pH on the stability of enzyme−nucleic acid complexes. X-ray diffraction analysis of the H12A and H119A variants at a resolution of 1.7 and 1.8 Å, respectively, shows that the amino acid substitutions do not perturb the overall structure of the variants. Isothermal titration calorimetric studies on the complexation of wild-type RNase A and the variants with 3′-UMP at pH 6.0 show that His12 and His119 contribute 1.4 and 1.1 kcal/mol to complex stability, respectively. Determination of the stability of the complex of wild-type RNase A and 6-carboxyfluorescein∼d(AUAA) at varying pHs by fluorescence anisotropy shows that the stability increases by 2.4 kcal/mol as the pH decreases from 8.0 to 4.0. At pH 4.0, replacing His12 with an alanine residue decreases the stability of the complex with 6-carboxyfluorescein∼d(AUAA) by 2.3 kcal/mol. Together, these structural and thermodynamic data provide the first thorough analysis of the contribution of histidine residues to nucleic acid binding.

Ribonuclease A (RNase A;[1] EC 3.1.27.5) is a pyrimidine-specific endoribonuclease from bovine pancreas. Decades of study have made this enzyme one of the most important model systems in enzymology and protein chemistry (*1*, *2*). RNase A depolymerizes an RNA substrate by cleaving a P−$O^{5'}$ bond after a pyrimidine base. The mechanism of the cleavage reaction catalyzed by RNase A employs two renowned histidine residues, His12 and His119 (*3*, *4*). In the transphosphorylation reaction, His12 acts as a base to abstract a proton from the 2′-hydroxyl group of a ribose ring, and His119 acts as an acid to donate a proton to the 5′-oxygen of the leaving group (Figure 1A). The roles of His12 and His119 as a base and an acid are switched in the subsequent hydrolysis reaction of 2′,3′-cyclic nucleotide substrates (Figure 1B) (*5*, *6*). Replacing either histidine residue with an alanine greatly impairs the catalytic activity of the enzyme. The k_{cat}/K_M values of the H12A and H119A variants for cleavage of UpA are $>10^4$-fold less than that of wild-type RNase A (*7*). Catalysis by RNase A requires another active site residue, Lys41. Lys41 facilitates catalysis by donating a hydrogen bond to a phosphoryl oxygen in the transition state (*8*). Replacing Lys41 with an alanine residue likewise decreases the k_{cat}/K_M value for cleavage of UpA by $>10^4$-fold (*9*).

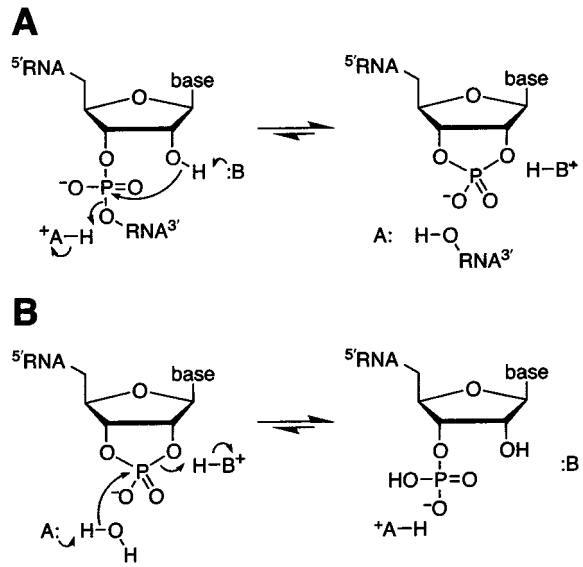

FIGURE 1: Putative mechanism of catalysis by ribonuclease A (*3*, *4*). (A) Transphosphorylation reaction. (B) Hydrolysis reaction. In both panels, B and A refer to His12 and His119, respectively.

The interaction of RNase A with single-stranded RNA extends beyond the enzymic active site. Phosphoryl group binding sites in RNase A have been identified and studied in detail by X-ray crystallography (*10*, *11*) and site-directed

† This work was supported by Grant GM44783 (NIH).

* To whom correspondence should be addressed at the Department of Biochemistry, University of Wisconsin−Madison, 433 Babcock Drive, Madison, WI 53706-1544. Telephone: (608) 262-8588. Fax: (608) 262-3453. E-mail: Raines@biochem.wisc.edu.

‡ Department of Biochemistry.

§ Present address: Hauptman-Woodward Medical Research Institute, 73 High St., Buffalo, NY 14203-1196.

|| Department of Chemistry.

[1] Abbreviations: 3′-UMP, uridine 3′-phosphate; 6-FAM, 6-carboxyfluorescein; cUMP, uridine 2′,3′-cyclic phosphate; K_a, acid dissociation constant; K_d, equilibrium dissociation constant; MES, 2-morpholinoethanesulfonic acid; MOPS, 3-morpholinopropanesulfonic acid; PDB, Protein Data Bank (http://www.rcsb.org/pdb/); rms, root mean square; RNase A, bovine pancreatic ribonuclease A; Tris, tris(hydroxymethyl)-aminomethane; UpA, uridylyl(3′→5′)adenosine.

10.1021/bi0100182 CCC: $20.00
Published on Web 03/29/2001

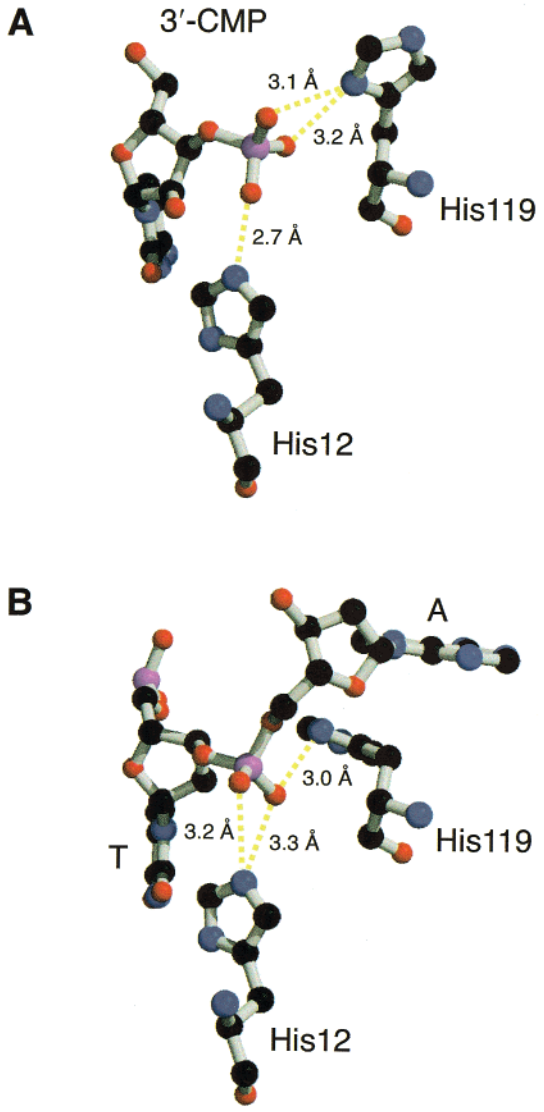

FIGURE 2: Interactions between the active site histidine residues of ribonuclease A and the phosphoryl group of a bound nucleic acid. (A) 3′-CMP [PDB entry 1RPF (*13*)]. (B) d(ATAAG) [PDB entry 1RCN (*8*)]. In both panels, hydrogen bonds formed by histidine residues and nonbridging oxygens are depicted as dashed yellow lines. Structures were created with the program MOLSCRIPT (*33*) and rendered with the program RASTER3D (*34*). Only the two underlined residues of d(ATAAG) are shown in panel B.

mutagenesis (*12*−*14*). These binding sites are composed of cationic residues that use Coulombic forces to attract the anionic phosphoryl groups of a nucleic acid (*15*). The active site residues comprise one of the phosphoryl group binding sites, P1 (Figure 2). Arg85 and Lys66 comprise the P(−1) and P0 site, respectively. Lys7 and Arg10 comprise the P2 site.

Physical characterization of complex formation by wild-type RNase A implicates the involvement of active site residues in phosphoryl group binding. The structure of crystalline complexes of wild-type RNase A and nucleic acids shows that the active site histidine residues are proximal to the phosphoryl group bound in the active site (*11*, *16*) (Figure 2). The stability of the complex of wild-type RNase A and cytidine 3′-phosphate (3′-CMP) is sensitive to the ionization state of these histidine residues (*17*−*19*). Binding of uridine 3′-phosphate (3′-UMP) to wild-type RNase A alters the microscopic pK_a values of the histidine residues, as revealed by NMR spectroscopy (*20*).

Here, we seek a quantitative assessment of the contribution of His12 and His119 to nucleic acid binding by RNase A. First, we use X-ray crystallography to assess the integrity of the structure of enzymic variants in which a histidine residue is replaced with alanine. Then, we characterize in detail the thermodynamics of complex formation by wild-type RNase A and the histidine variants by using isothermal titration calorimetry, fluorescence anisotropy, and pH titration. The results provide a thorough picture of the interaction of two histidine residues with a nucleic acid.

MATERIALS AND METHODS

Materials. Wild-type RNase A and the H12A and H119A variants were produced, folded, and purified as described elsewhere (*21*, *22*). Concentrations of wild-type RNase A and its variants were determined by ultraviolet spectroscopy using $\epsilon = 0.72$ mL mg^{-1} cm^{-1} at 277.5 nm (*23*). 6-Carboxyfluorescein∼d(AUAA) [6-FAM∼d(AUAA)] was from Promega (Madison, WI). The concentration of 6-FAM∼d(AUAA) was determined by using $\epsilon = 66\,250$ M^{-1} cm^{-1} at 260 nm (*24*). 3′-UMP was from Sigma Chemical Co. (St. Louis, MO). The concentration of 3′-UMP was determined by using $\epsilon = 10\,000$ M^{-1} cm^{-1} at 260 nm (*25*).

Protein Crystallization. Crystals of H12A and H119A RNase A were prepared by vapor diffusion using the hanging drop method. Drops (6 μL) of 0.050 M sodium acetate buffer (pH 6.0), containing H12A RNase A (33 mg/mL), saturated sodium chloride (25% v/v), and saturated ammonium sulfate (15% v/v), were suspended over 1.0 mL wells of 0.10 M sodium acetate buffer (pH 6.0) containing saturated sodium chloride (50% v/v) and saturated ammonium sulfate (30% v/v). Single trigonal crystals were grown at 20 °C, appeared within several weeks, and grew to a final size of 0.6 × 0.6 × 0.5 mm.

Drops (6 μL) of 0.050 M sodium acetate buffer (pH 6.0), containing H119A RNase A (30 mg/mL), saturated sodium chloride (22.5% v/v), and saturated ammonium sulfate (14.5% v/v), were suspended over 1.0 mL wells of 0.10 M sodium acetate buffer (pH 6.0) containing saturated sodium chloride (45% v/v) and saturated ammonium sulfate (29% v/v). Single trigonal crystals were grown at 20 °C, appeared within 1 week, and grew to a final size of 0.6 × 0.6 × 0.6 mm.

X-ray Diffraction Data Collection. Crystals of H12A RNase A were of space group $P3_221$, with $a = 64.54$ Å, $c = 65.08$ Å, $\alpha = \beta = 90°$, and $\gamma = 120°$. Crystals of H119A RNase A were of space group $P3_221$, with $a = 64.53$ Å, $c = 65.04$ Å, $\alpha = \beta = 90°$, and $\gamma = 120°$. All X-ray data were collected with a Siemens HI-STAR detector mounted on a Rigaku rotating anode operating at 50 kV and 90 mA with a 300 μm focal spot. The X-ray beam was collimated by double-focusing mirrors. The crystal-to-detector distance was 12.0 cm. Data were obtained in 512 × 512 pixel format, processed with the program XDS (*26*, *27*), and scaled with the program XSCALIBRE (G. Wesenberg and I. Rayment, unpublished results). For each protein, frames of data (135°) were collected from a single crystal by using a combination of ω and ϕ scans. Reflections with $I/\sigma < 0.33$ were rejected.

Table 1: X-ray Diffraction Analysis Statistics of H12A Ribonuclease A

crystal data	H12A RNase A
space group	$P3_221$
cell dimensions (Å)	$a = 64.54$ (1)
	$b = 64.54$ (1)
	$c = 65.08$ (2)
protein molecules/unit cell	6
data collection statistics	
resolution (Å)	1.7
no. of measured reflections ($I/\sigma > 0.33$)	50643
no. of unique reflections	20142
average redundancy	2.5
average I/σ	24
completeness (30−1.7) (%)	96
completeness high-resolution shell (%)	(1.8−1.7 Å) 88
R_{sym}	0.030
R_{sym} high-resolution shell	(1.8−1.7 Å) 0.13
final refinement statistics	
H12A RNase A atoms	960
solvent atoms	99
R-factor	(30−1.7 Å) 0.182
RMS deviation from ideal geometry	
bond distances (Å)	0.012
bond angles (deg)	2.31
average *B*-factors (Å^2)	
main-chain atoms	30.4
side-chain atoms	36.7
chloride atoms	32.6

Table 2: X-ray Diffraction Analysis Statistics of H119A Ribonuclease A

crystal data	H119A RNase A
space group	$P3_221$
cell dimensions (Å)	$a = 64.53$ (1)
	$b = 64.53$ (1)
	$c = 65.04$ (2)
protein molecules/unit cell	6
data collection statistics	
resolution (Å)	1.8
no. of measured reflections ($I/\sigma > 0.33$)	68047
no. of unique reflections	23009
average redundancy	3.0
average I/σ	19
completeness (30−1.8) (%)	94
completeness high-resolution shell (%)	(1.9−1.8 Å) 90
R_{sym}	0.033
R_{sym} high-resolution shell	(1.9−1.8 Å) 0.149
final refinement statistics	
H119A RNase A atoms	960
solvent atoms	99
R-factor	(30−1.8 Å) 0.164
RMS deviation from ideal geometry	
bond distances (Å)	0.011
bond angles (deg)	2.41
average *B*-factors (Å^2)	
main-chain atoms	25.5
side-chain atoms	32.1
chloride atoms	29.5

The crystals were cooled in a 2 °C air stream, resulting in negligible crystal decay for both data collections. Full crystallographic details are listed in Tables 1 and 2.

Refinement of the H12A Structure. The structure was solved by using difference Fourier maps with PDB entry 4RSD (*28*), stripped of solvent, as a starting model (Ala121 was replaced by Asp and His12 by Ala). A rigid body refinement resulted in an *R*-factor of 0.369. Prior to least-squares refinement $2|F_o| - |F_c|$, $|F_o| - |F_c|$, and σ_A (*29*), difference maps were calculated by using the data from 30 to 3.0 Å. The model (residues 1−11 and 13−124) was examined and was continuous in electron density for the entire chain. Residue 12 was identified clearly as alanine. The starting model was subjected to 10 cycles of least-squares refinement with the program TNT (*30*) and the data from 30 to 2.0 Å, giving an initial *R*-factor of 0.238. Manual adjustments to the model were performed with the program TURBO−FRODO (*31*). The resolution was extended to 1.7 Å after several cycles of manual adjustments and least-squares refinement. The peak-searching algorithm in TNT was used to place ordered water molecules. Water molecules were retained if they had at least 1σ of $2|F_o| - |F_c|$ density, 3σ of $|F_o| - |F_c|$ density, and were within hydrogen-bonding distance of the protein or other water molecules. The final model contains the complete protein (residues 1−124), 96 water molecules, and two chloride ions.

Refinement of the H119A Structure. The structure was solved by using difference Fourier maps with PDB entry 4RSD (*28*), stripped of solvent, as a starting model (Ala121 was replaced by Asp and His119 by Ala). A rigid body refinement resulted in an *R*-factor of 0.345. Prior to least-squares refinement $2|F_o| - |F_c|$, $|F_o| - |F_c|$, and σ_A (*29*), difference maps were calculated by using the data from 30 to 3.0 Å. The model (residues 1−118 and 120−124) was examined and was continuous in the density for the entire chain. Residue 119 was identified clearly as alanine. The starting model was subjected to 10 cycles of least-squares refinement with the program TNT (*30*) and the data from 30 to 2.0 Å, giving an initial *R*-factor of 0.220. Manual adjustments to the model were performed with the program TURBO−FRODO (*31*). The resolution was extended to 1.8 Å after several cycles of manual adjustments and least-squares refinement. Water molecules from the H12A structure were used as a starting solvent model. Water molecules were retained if they had at least 1σ of $2|F_o| - |F_c|$ density, 3σ of $|F_o| - |F_c|$ density, and were within hydrogen-bonding distance of the protein or other water molecules. The final model contains the complete protein (residues 1−124), 102 water molecules, and three chloride ions.

Atomic coordinates for H12A RNase A and H119A RNase A have been deposited in the PDB with accession codes 1C9V and 1C9X, respectively.

Determination of K_d for RNase A−3′-UMP Complexes. The stability of the complexes of 3′-UMP with wild-type RNase A and the H12A and H119A variants was determined by isothermal titration calorimetry using a Micro Calorimetry System from MicroCal (Northampton, MA). The proteins and 3′-UMP solutions were prepared with 0.10 M MES−NaOH (pH 6.0), containing 0.10 M NaCl, and were degassed prior to use. The volume of protein solution in the sample cell of the calorimeter was 1.3 mL. For wild-type RNase A, the initial concentration of protein in the cell was 0.12 mM. Aliquots (5.0 μL) of 2.8 mM 3′-UMP solution were injected into the cell at 240 s intervals. For the H12A and H119A variants, the initial concentration of protein in the cell was 0.64 and 0.65 mM, respectively. Aliquots (5.0 μL) of 22 mM 3′-UMP were injected into the cell at 240 s intervals. The heat evolved from complex formation was recorded and analyzed to determine K_d values with the program ORIGIN (MicroCal Software, Northampton, MA) (*32*).

Determination of K_d for RNase A−6-FAM∼d(AUAA) Complexes at Varying pHs. The stability of the complex

Table 3: Thermodynamic Stability of Complexes of 3′-UMP with Wild-Type Ribonuclease A and the H12A and H119A Variants

ribonuclease A	K_d (mM)[a]	$\Delta G°$ (kcal/mol)[b]
wild type	0.054	−5.8
H12A	0.55	−4.4
H119A	0.37	−4.7

[a] Values were obtained by using isothermal titration calorimetry at 25 °C in 0.10 M MES−NaOH buffer (pH 6.0) containing 0.10 M NaCl. [b] $\Delta G° = RT \ln(K_d/M)$.

between RNase A and an oligonucleotide was determined by fluorescence anisotropy using a Beacon Fluorescence Polarization System from PanVera (Madison, WI). The ligand, 6-FAM∼d(AUAA), is a DNA oligonucleotide with a fluorescein moiety attached to its 5′-end via a 6-carbon spacer (*14*, *33*). Wild-type RNase A was prepared in 2.0 mL of buffers with pH 4.0−8.0, as listed in Table 4. H12A RNase A was prepared in 2.0 mL of 0.10 M sodium acetate buffer (pH 4.0) containing 0.050 M NaCl. Determination of the K_d values of the complex of H12A RNase A and 6-FAM∼d(AUAA) at a pH other than 4.0 [or H119A RNase A and 6-FAM∼d(AUAA) at any pH] was not possible with this method because of the low affinity of the variant for the ligand. The buffers used for this study were designed to have an identical ionic strength of 0.15. The solutions of protein were divided to prepare 1.0 mL of both a sample solution and a blank solution in silanized borosilicate glass tubes. Both solutions contained the same concentration of wild-type RNase A (1.9−3.4 mM) or H12A RNase A (5.7 mM), but only the sample solution contained ligand (2.5−5.0 nM). Fluorescence anisotropy was measured at 23 °C with excitation at 488 nm and emission at 520 nm. Anisotropy values of the sample solution were determined five times with a blank reading before each sample reading. After each measurement, the sample solution was diluted by removing 0.25 mL of the sample and adding 0.25 mL of buffer containing the same concentration of the ligand as the sample solution to reduce protein concentration for subsequent measurements. The blank solution was also diluted with buffer by the same procedure. The measurement was continued until the anisotropy values approached a minimum. Equilibrium dissociation constants at each pH were determined with the equation:

$$A = \frac{\Delta A[\text{RNase A}]}{K_d + [\text{RNase A}]} + A_{min} \quad (1)$$

where A_{min} is the anisotropy of free ligand and ΔA is the difference in anisotropy between free ligand and bound ligand. Nonlinear regression analyses of the data were performed with the program SIGMAPLOT 5.0 (SPSS, Chicago, IL).

RESULTS

Structure of H12A RNase A. The structure of H12A RNase A was solved by difference Fourier analysis and refined to an *R*-factor of 0.182 using data from 30 to 1.7 Å. The RMS deviation from target geometries is 0.012 Å for bond lengths and 2.31° for bond angles. The average *B*-factor for the main chain and side chain is 30.4 and 36.7 Å^2, respectively. The electron density is continuous for the main chain and most of the side chains. The conformation of residue 12 was unambiguous and clearly defined in both $2|F_o| - |F_c|$ density and annealed omit $|F_o| - |F_c|$ density (Figure 3A).

Structure of H119A RNase A. The structure of H119A RNase A was solved by difference Fourier analysis and refined to an *R*-factor of 0.164 using data from 30 to 1.8 Å. The RMS deviation from target geometries is 0.011 Å for bond lengths and 2.41° for bond angles. The average *B*-factor for the main chain and side chain is 25.5 and 32.1 Å^2, respectively. The electron density is continuous for the main chain and most of the side chains. The conformation of residue 119 was unambiguous and clearly defined in both $2|F_o| - |F_c|$ density and annealed omit $|F_o| - |F_c|$ density (Figure 3B).

Binding of 3′-UMP to Wild-Type RNase A and the H12A and H119A Variants. To assess the role of the two active site histidine residues in binding to 3′-UMP, the values of the equilibrium dissociation constant (K_d) of the enzymic complexes with ligand were determined by using isothermal titration calorimetry (Table 3). The K_d of the complex of wild-type RNase A and 3′-UMP was 0.054 mM, which is identical to a value reported previously (*34*). The K_d's for H12A RNase A and H119A RNase A with the same ligand were 0.55 and 0.37 mM, respectively. These increases in K_d value correspond to decreases in the stability of the H12A and H119A complexes of 1.4 and 1.1 kcal/mol, respectively.

Stability of the RNase A−6-FAM∼d(AUAA) Complex. The effect of pH on the stability of the complex of RNase A and an oligonucleotide was determined by using fluorescence anisotropy. The values of K_d for the complex with 6-FAM∼d(AUAA) were obtained at pH 4.0−8.0 (Table 4). The stability of the complex was maximal at acidic pH. As the pH was increased, the K_d of the complex also increased. At pH 8.0, the K_d was ∼60-fold higher than the K_d determined at pH 4.0. The K_d value of the complex with H12A RNase A (2.0 ± 0.4 mM) at pH 4.0 was significantly greater than that for the complex with wild-type RNase A (0.038 ± 0.005 mM).

Table 4: Thermodynamic Stability of the Complexes of 6-FAM∼d(AUAA) with Wild-Type Ribonuclease A and the H12A Variant

RNase A	pH	buffer condition	K_d (mM)[a]	$\Delta G_{binding}°$ (kcal/mol)[c]
wild type	4.0	0.10 M NaOAc−HCl, 0.050 M NaCl	0.038 ± 0.005	−5.99 ± 0.08
	5.0	0.10 M NaOAc−HCl, 0.050 M NaCl	0.040 ± 0.002	−5.96 ± 0.03
	6.0	0.10 M MES−NaOH, 0.10 M NaCl	0.088 ± 0.008[b]	−5.50 ± 0.05
	7.2	0.10 M MOPS−NaOH, 0.10 M NaCl	1.1 ± 0.1	−4.01 ± 0.05
	8.0	0.10 M Tris-HCl−NaOH, 0.050 M NaCl	2.2 ± 0.2	−3.60 ± 0.05
H12A	4.0	0.10 M NaOAc−HCl, 0.050 M NaCl	2.0 ± 0.4	−3.7 ± 0.1

[a] Values (±SE) were obtained by using fluorescence anisotropy at 23 °C in the designated buffer. [b] Data from ref *29*. [c] $\Delta G° = -RT \ln(K_d/M)$.

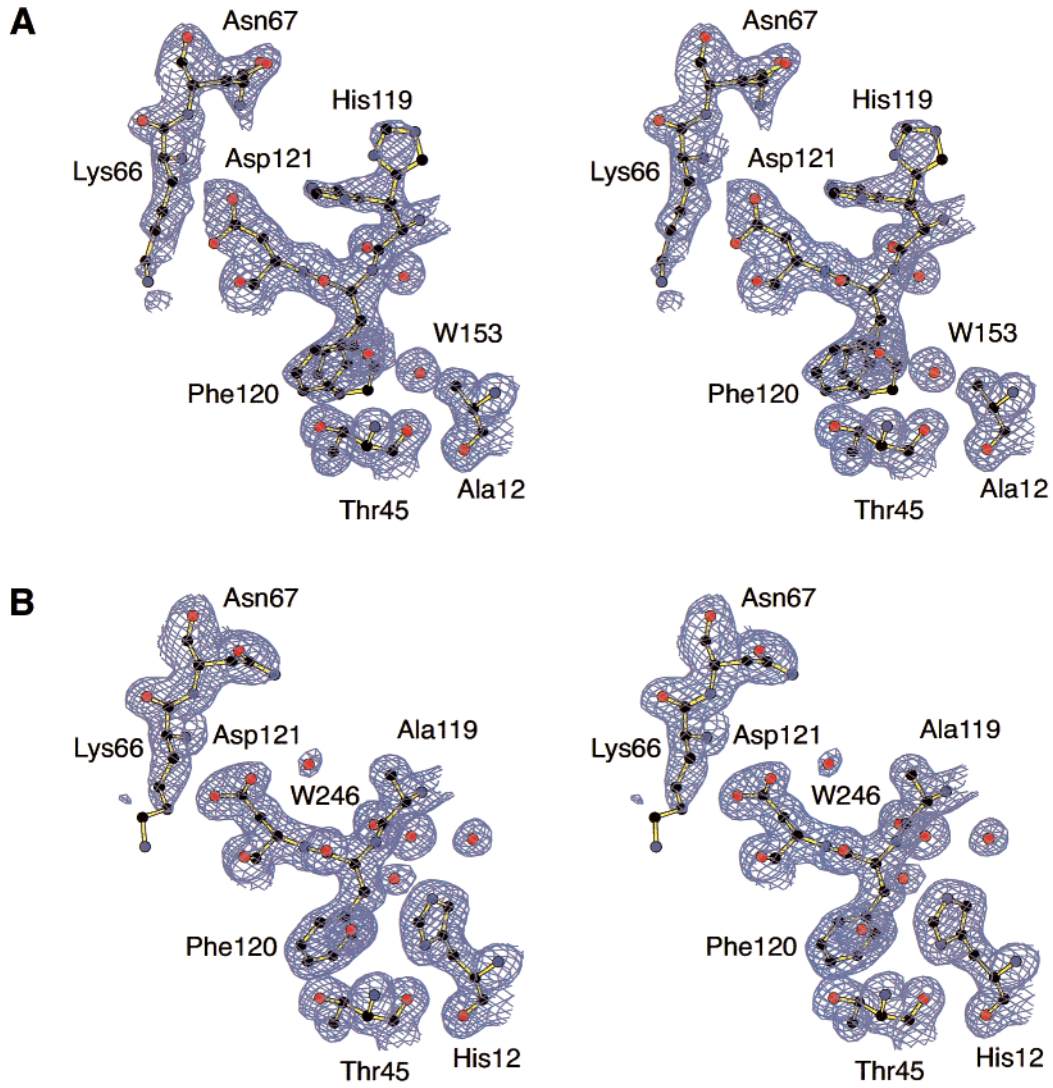

FIGURE 3: Stereoviews of the active site of crystalline H12A ribonuclease A and crystalline H119A ribonuclease A. The electron density is $2|F_o| - |F_c|$ contoured at 1.0σ. (A) H12A ribonuclease A. Loss of the side chain at residue 12 creates disorder in residues Asn67, His119, and Phe120. A water molecule (W153) is occupying the position of the side chain of His12. (B) H119A ribonuclease A. Loss of the side chain at residue 119 has little effect on the structure. A water molecule (W246) forms a hydrogen bond with the side chain of Asp121 in place of the side chain of His119.

DISCUSSION

Structural Comparison of Wild-Type RNase A and the H12A and H119A Variants. H12A RNase A and H119A RNase A have structures that are almost identical overall to that of the wild-type enzyme. The main-chain atoms of the H12A and H119A variants have an average RMS deviation of 0.31 and 0.24 Å from those of wild-type RNase A [PDB entry 1RPH (*16*)]. The main-chain conformations of Ala12 and Ala119 are similar to those of the analogous residues in wild-type RNase A. H12A RNase A shows the greatest deviations, which occur in residues 66 and 67, with the main chain deviating up to 0.5 Å.

Active Site Structure in H12A RNase A and H119A RNase A. In H12A RNase A, a water molecule (W153) occupies the position of the imidazole ring of His12 in wild-type RNase A. W153 forms a hydrogen bond to the main-chain O of Thr45 (2.95 Å) that is analogous to the hydrogen bond formed between $N_{\delta 1}$ of His12 and the main-chain O of Thr45 in the wild-type enzyme. W153 is part of a water network in the active site and is within hydrogen-bonding distance of W195 (2.79 Å), a solvent molecule that is replaced by a chloride ion in the structure of H119A RNase A as well as T45G RNase A (*33*). His12 occupies a similar position in wild-type RNase A and the H119A variant.

In H12A RNase A, the electron density surrounding the side chain of His119 is diffuse due to some disorder in this residue. Although it was possible to define χ_1, it was difficult to assess χ_2 because of weak electron density. His119 occupies two positions in the H12A RNase A structure, commonly defined as "A" and "B" (*35*). In wild-type RNase A, the A position brings the side-chain $N_{\epsilon 2}$ of His119 within hydrogen-bonding distance of the side-chain $O_{\delta 1}$ of Asp121 (2.97 Å), and $O_{\delta 2}$ of Asp121 forms a hydrogen bond with the main-chain N of Lys66 (3.35 Å). In H12A RNase A, however, a shift of the Asp121 side chain puts the side-chain $N_{\epsilon 2}$ of His119 3.71 Å from the side-chain $O_{\delta 1}$ of Asp121. Instead, $O_{\delta 1}$ of Asp121 is involved in a hydrogen bond with the main-chain N of Lys66 (3.03 Å). These conformational changes may have resulted in the 0.5 Å shift of residues 66 and 67 away from the active site with respect to wild-type

Scheme 1

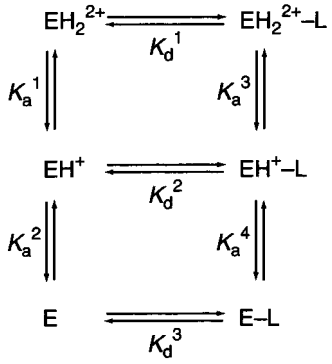

RNase A. In H119A RNase A, a water molecule (W246) forms a hydrogen bond with the side-chain $O_{\delta 1}$ of Asp121 (2.74 Å), replacing the His119 side chain. $O_{\delta 2}$ of Asp121 forms a hydrogen bond with the main-chain N of Lys66 (3.12 Å).

In wild-type RNase A, the side chain of Phe120 is in contact with the side chain of His12. In the H12A RNase A structure, Phe120 becomes slightly disordered and occupies two distinct positions (χ_1, χ_2 angles of −174°, 97° and −140°, 128°). The first position is similar to that of Phe120 in wild-type RNase A (χ_1, χ_2 angles of −164°, 93°); the second position fills space vacated by the absence of the side chain at residue 12.

Effects of Ionization of His12 and His119 on Nucleic Acid Binding. The K_d value of the RNase A−6-FAM∼d(AUAA) complex was determined at varying pHs. DNA oligonucleotides have been used previously as substrate analogues for crystallographic and biophysical studies of RNase A (*15*, *11*). Specifically, the effect of pH on ligand binding has been studied with 3′-UMP (*17*−*19*). This analysis was not straightforward because of the titration of the ligand near pH 6. The use of a DNA oligonucleotide as a ligand obviates this complication, as the ionization state of the phosphoryl groups of DNA is constant in the range of pH used for this study. Within this range of pH, we assume that the only titratable groups affecting the K_d value are those of His12 and His119. Scheme 1 shows a general thermodynamic cycle for ligand binding with macroscopic acid dissociation constants and K_d values.

In Scheme 1, K_a^1 and K_a^2 are macroscopic acid equilibrium constants for the free enzyme, K_a^3 and K_a^4 are macroscopic acid dissociation constants for the enzyme bound to the ligand, and K_d^1, K_d^2, and K_d^3 are equilibrium dissociation constants for each complex of the ligand and the enzyme with its different ionization status. Given this thermodynamic cycle, the apparent equilibrium dissociation constant, $K_{d,app}$, can be written:

$$K_{d,app} = K_d^1 \left(\frac{1 + \frac{K_a^1}{[H^+]} + \frac{K_a^1 K_a^2}{[H^+]^2}}{1 + \frac{K_a^3}{[H^+]} + \frac{K_a^3 K_a^4}{[H^+]^2}} \right) \quad (2)$$

Microscopic pK_a values for His12 and His119 have been determined by NMR spectroscopy to be 5.64 ± 0.03 and 5.91 ± 0.04, respectively, when the other is unprotonated (*31*). To reduce the number of parameters, the K_a values of His12 and His119 are assumed to be identical. This approximation is valid here, as the data in Table 4 cannot accurately resolve the small difference in the pK_a values of His12 and His119. By assigning K_a of His12 and His119 as K_a^f in the free enzyme and K_a^b in the bound enzyme, the four macroscopic acid equilibrium constants, K_a^1, K_a^2, K_a^3, and K_a^4 in eq 2 can be expressed as $2K_a^f$, $K_a^f/2$, $2K_a^b$, and $K_a^b/2$ (*32*). Then, eq 2 can be rewritten:

$$K_{d,app} = K_d^1 \left(\frac{1 + \frac{2K_a^f}{[H^+]} + \left(\frac{K_a^f}{[H^+]}\right)^2}{1 + \frac{2K_a^b}{[H^+]} + \left(\frac{K_a^b}{[H^+]}\right)^2} \right) \quad (3)$$

which can be converted into an equation for free energy as a function of pH:

$$\Delta G_{binding}^\circ = \Delta G^1 + RT \ln\left(\frac{1 + 2(10^{pH - pK_a^f}) + 10^{2(pH - pK_a^f)}}{1 + 2(10^{pH - pK_a^b}) + 10^{2(pH - pK_a^b)}} \right) \quad (4)$$

In eq 4, $\Delta G_{binding}^\circ$ is the change in free energy at each pH and ΔG^1 is the change in the free energy when the histidine residues are fully protonated (corresponding to K_d^1 in Scheme 1). A fit of the data in Table 4 is shown in Figure 4. The values of pK_a^f and pK_a^b are thus determined to be 6.14 ± 0.03 and 7.08 ± 0.03, respectively, and ΔG^1 is determined to be −6.03 ± 0.02 kcal/mol. From these parameters, $\Delta G^1 - \Delta G^3$, the difference between the complex stability in its protonated form (ΔG^1) and that in its unprotonated form (ΔG^3, corresponding to K_d^3 in Scheme 1) is calculated to be −2.5 ± 0.1 kcal/mol. Hence, the protonation of each histidine residue contributes approximately 1.2 kcal/mol to the stability of the complex.

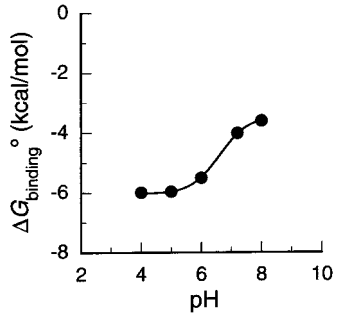

FIGURE 4: Effect of pH on the stability of the wild-type ribonuclease A−6-FAM∼d(AUAA) complex. Nonlinear regression of the data with eq 4 yields pK_a^f = 6.14 ± 0.03, pK_a^b = 7.08 ± 0.03, and ΔG^1 = −6.03 ± 0.02 kcal/mol.

The increase in the pK_a values of the active site histidine residues suggests that the binding of the ligand stabilizes the imidazolium form of the side chain by Coulombic interactions. The microscopic pK_a values of the histidine residues have been shown to increase by 0.5−0.8 unit upon binding to 3′-UMP (*17*). The macroscopic pK_a's determined from pH−k_{cat}/K_M and pH−k_{cat} profiles also have shown that the binding of substrate to the active site of RNase A increases the pK_a values of these histidine residues (*3*, *28*).

Effect of Replacing Active Site Histidine Residues on Nucleic Acid Binding. The effect of replacing the active site

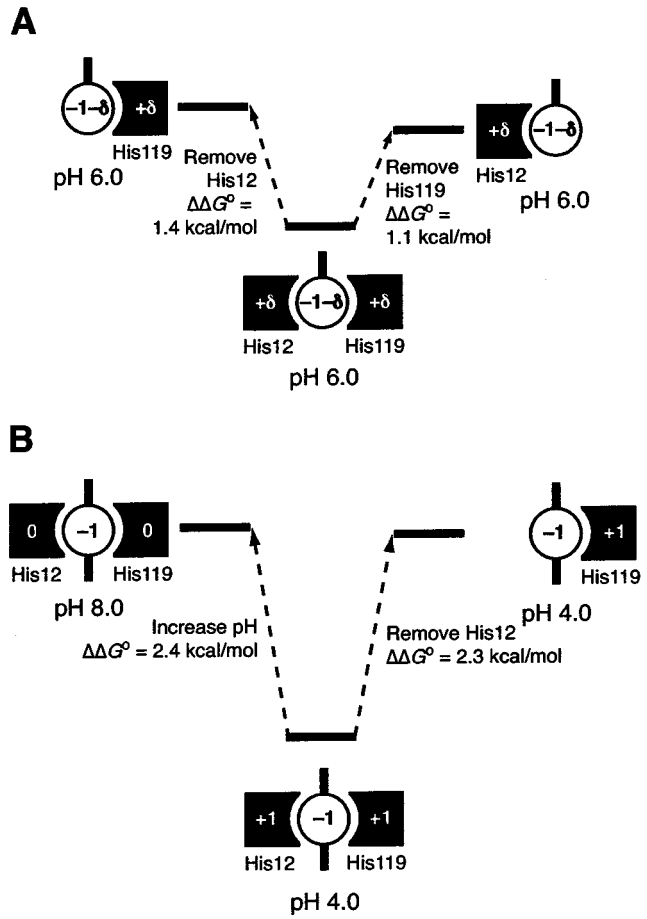

FIGURE 5: Diagrams depicting the contribution of the active site histidine residues of ribonuclease A to nucleic acid binding. (A) Complex with 3′-UMP. (B) Complex with 6-FAM∼d(AUAA). In both panels, phosphoryl groups are depicted as circles, His12 and His119 are depicted as squares with a concave surface facing a phosphoryl group, and numbers in shapes refer to formal charges with δ referring to a partial charge.

histidine residues on nucleic acid binding is depicted in Figure 5. When wild-type RNase A forms a complex with 3′-UMP at pH 6.0, the active site histidine residues form Coulombic interactions with the phosphoryl group of 3′-UMP. When His12 or His119 is replaced with an alanine residue, the complex stability is decreased by 1.4 or 1.1 kcal/mol, respectively (Figure 5A). Direct assignment of the decrease in stability to specific interactions is not feasible because of the partial protonation states of the histidine residues and 3′-UMP at pH 6.0.

The substitution of His12 with an alanine residue also affects the stability of the complex with 6-FAM∼d(AUAA). At pH 4.0, where the complex with wild-type RNase A is most stable, the K_d for the complex with H12A RNase A is 2.0 ± 0.4 mM. The $\Delta G_{binding}°$ was calculated to be −3.7 ± 0.1 kcal/mol, which is 2.3 kcal/mol greater than that of the complex with wild-type RNase A at the same pH. This $\Delta G_{binding}°$ of the complex with H12A RNase A at pH 4.0 is comparable to that of the complex with wild-type RNase A at pH 8.0 (Figure 5B). When the pH is increased from 4.0 to 8.0, the wild-type RNase A−6-FAM∼d(AUAA) complex becomes less stable by 2.4 kcal/mol, or 1.2 kcal/mol per histidine residue. When protonated His12 is replaced with an alanine residue, the complex loses 2.3 kcal/mol in stability. Therefore, the neutral His12 still contributes ∼1.1 kcal/mol to the stability of the complex at pH 8.0. These energetic considerations imply that the interaction between His12 and the nucleic acid at pH 4.0 relies not only on a hydrogen bond between the cationic imidazolium group and an anionic nonbridging oxygen but also on interactions that even a neutral imidazole group and a nucleic acid can form at pH 8.0 (vide infra).

The contribution of the imidazolium form of His12 to complex stability, 2.3 kcal/mol, is prominent. Lys66 and Lys7/Arg10 comprise the enzymic P0 and P2 subsites, respectively. Like His12, Lys66 and Lys7/Arg10 interact with a phosphoryl group of a bound nucleic acid (*10*). K66A RNase A forms a complex that is 0.9 kcal/mol less stable than that of the wild-type enzyme in a similar solution condition (0.10 M MES−NaOH buffer, pH 6.0, containing 0.10 M NaCl). K7A/R10A RNase A forms a complex that is 1.2 kcal/mol less stable in this solution condition. Thus, the contribution of protonated His12 to binding is greater by 1.1−1.4 kcal/mol than that of either the P0 or the P2 subsite.

Interaction of Active Site Histidine Residues with Nucleic Acids. The structure of the crystalline wild-type RNase A−3′-CMP complex [PDB entry 1RPF (*13*)] shows that His12 and His119 are both within hydrogen-bonding distance of the phosphoryl group of 3′-CMP (Figure 2A). Specifically, $N_{\epsilon 2}$ of His12 is 2.7 Å from an oxygen of the phosphoryl group of 3′-CMP, and $N_{\delta 1}$ of His119 is 3.1 Å from another oxygen. Rotation about the $P-O^{3'}$ bond of the 3′-CMP molecule varies the lengths of these hydrogen bonds. In the structure of the crystalline complex of K7A/R10A/K66A RNase A and 3′-UMP [PDB entry 4RSK (*29*)], $N_{\epsilon 2}$ of His12 does form a longer hydrogen bond with a phosphoryl oxygen (3.0 Å), and $N_{\delta 1}$ of His119 forms a shorter hydrogen bond (2.7 Å).

The structure of the crystalline complex of wild-type RNase A and d(ATAAG) [PDB entry 1RCN (*8*)] provides insight into the stability of the RNase A−6-FAM∼d(AUAA) complex (Figure 2B). In the wild-type RNase A−d(ATAAG) complex, $N_{\epsilon 2}$ of His12 is within hydrogen-bonding distance of two nonbridging oxygens of the ligand, 3.2 Å from one and 3.3 Å from another. Likewise, $N_{\delta 1}$ of His119 forms hydrogen bonds with a nonbridging oxygen and 5′-oxygen of the phosphoryl group in the active site, each with a length of 3.0 Å.[2] Protonation of His12 or His119 adds a Coulombic component that strengthens all of these hydrogen bonds in a manner consistent with the pH dependence of complex stability (Figure 4). The side chain of His12 is also in contact with the thymine nucleobase of the ligand. Likewise, the side chain of His119 stacks with an adenine nucleobase. These hydrophobic interactions could be responsible for the favorable contribution of the imidazole form of His12 and His119 to complex stability as well as for making the contribution of the active site histidines greater than that of the P0 and P2 subsites (*10*).

Implications for Catalysis by RNase A. The important role of His12 and His119 of RNase A in nucleic acid binding has a noteworthy implication for nucleic acid turnover. Because the transphosphorylation reaction catalyzed by RNase A requires His12 to act as a base (Figure 1A), catalysis is impaired at acidic pH (*3*, *28*). Nucleic acid

[2] $N_{\delta 1}$ of His12 and $N_{\epsilon 2}$ of His119 donate hydrogen bonds to the main-chain oxygen of Thr45 and a side-chain oxygen of Asp121, respectively.

binding is, however, maximal at acidic pH (Table 4; Figure 4). Thus, enzyme−substrate complexes with improper ionization states of the active site histidines, which are nonproductive for substrate turnover, are prevalent at acidic pH and are likely to diminish catalytic efficacy.

ACKNOWLEDGMENT

We are grateful to Dr. J. E. Thompson for initiating the study of His12 and His119 of RNase A in our laboratory, to Dr. B. R. Kelemen for advice, and to Prof. I. Rayment, Prof. H. M. Holden, and the members of their research group for many helpful conversations and for the use of their X-ray data collection and computational facilities, which are supported by Grant BIR-9317398 (NSF). Calorimetry data were obtained at the University of Wisconsin−Madison Biophysical Instrumentation Facility, which is supported by the University of Wisconsin−Madison and Grants BIR-9512577 (NSF) and S10 RR13790 (NIH).

REFERENCES

1. D'Alessio, G., and Riordan, J. F. (1997) *Ribonucleases: Structure and Functions*, Academic Press, New York.
2. Raines, R. T. (1998) *Chem. Rev. 98*, 1045−1066.
3. Findlay, D., Herries, D. G., Mathias, A. P., Rabin, B. R., and Ross, C. A. (1961) *Nature 190*, 781−784.
4. Findlay, D., Herries, D. G., Mathias, A. P., Rabin, B. R., and Ross, C. A. (1962) *Biochem. J. 85*, 152−153.
5. Cuchillo, C. M., Parés, X., Guasch, A., Barman, T., Travers, F., and Nogués, M. V. (1993) *FEBS Lett. 333*, 207−210.
6. Thompson, J. E., Venegas, F. D., and Raines, R. T. (1994) *Biochemistry 33*, 7408−7414.
7. Thompson, J. E., and Raines, R. T. (1995) *J. Am. Chem. Soc. 116*, 5467−5467.
8. Messmore, J. M., Fuchs, D. N., and Raines, R. T. (1995) *J. Am. Chem. Soc. 117*, 8057−8060.
9. Messmore, J. M., and Raines, R. T. (2000) *J. Am. Chem. Soc. 122*, 9911−9916.
10. McPherson, A., Brayer, G., Cascio, D., and Williams, R. (1986) *Science 232*, 765−768.
11. Fontecilla-Camps, J. C., de Llorens, R., le Du, M. H., and Cuchillo, C. M. (1994) *J. Biol. Chem. 269*, 21526−21531.
12. Boix, E., Nogues, M. V., Schein, C. H., Benner, S. A., and Cuchillo, C. M. (1994) *J. Biol. Chem. 269*, 2529−2534.
13. Fisher, B. M., Grilley, J. E., and Raines, R. T. (1998) *J. Biol. Chem. 273*, 34134−34138.
14. Fisher, B. M., Ha, J.-H., and Raines, R. T. (1998) *Biochemistry 37*, 12121−12132.
15. Record, M. T., Jr., Lohman, M. L., and De Haseth, P. (1976) *J. Mol. Biol. 107*, 145−158.
16. Zegers, I., Maes, D., Dao-Thi, M. H., Poortmans, F., Palmer, R., and Wyns, L. (1994) *Protein Sci. 3*, 2322−2339.
17. Flogel, M., Albert, A., and Biltonen, R. L. (1975) *Biochemistry 14*, 2616−2621.
18. Flogel, M., and Biltonen, R. L. (1975) *Biochemistry 14*, 2603−2609.
19. Flogel, M., and Biltonen, R. L. (1975) *Biochemistry 14*, 2610−2615.
20. Quirk, D. J., and Raines, R. T. (1999) *Biophys. J. 76*, 1571−1579.
21. delCardayré, S. B., Ribo, M., Yokel, E. M., Quirk, D. J., Rutter, W. J., and Raines, R. T. (1995) *Protein Eng. 8*, 261−273.
22. Park, C., and Raines, R. T. (2000) *Protein Sci. 9*, 2026−2033.
23. Sela, M., Anfinsen, C. B., and Harrington, W. F. (1957) *Biochim. Biophys. Acta 26*, 502−512.
24. Wallace, R. B., and Miyada, C. G. (1987) *Methods Enzymol. 152*, 432−442.
25. Beaven, G. H., Holiday, E. R., and Johnson, E. A. (1955) in *The Nucleic Acids: Chemistry and Biology* (Chargaff, E., and Davison, J. D., Eds.) pp 493−553, Academic Press, New York.
26. Kabsch, W. (1988) *J. Appl. Crystallogr. 21*, 916−924.
27. Kabsch, W. (1998) *J. Appl. Crystallogr. 21*, 67−71.
28. Schultz, L. W., Quirk, D. J., and Raines, R. T. (1998) *Biochemistry 37*, 8886−8898.
29. Collaborative Computational Project, Number 4 (1994) *Acta Crystallogr. D50*, 760−763.
30. Tronrud, D. E., Ten-Eyck, L. F., and Matthews, B. W. (1987) *Acta Crystallogr. A43*, 489−501.
31. Cambillau, C., Roussel, A., Inisan, A. G., and Knoops-Mouthay, E. (1997) CNRS/Universite Aix-Marseille II, Marseille, France.
32. Wiseman, T., Williston, S., Brandts, J. F., and Lin, L.-N. (1989) *Anal. Biochem. 179*, 131−137.
33. Kelemen, B. R., Schultz, L. W., Sweeney, R. Y., and Raines, R. T. (2000) *Biochemistry 39*, 14487−14494.
34. Fisher, B. M., Schultz, L. W., and Raines, R. T. (1998) *Biochemistry 37*, 17386-17401.
35. Borkakoti, N., Moss, D. S., and Palmer, R. A. (1982) *Acta Crystallogr. B38*, 2210−2217.

BI0100182